Annular Contacts

10

In this chapter, we will turn our attention back to contact problems with an ideally elastic, homogeneous, isotropic half-space. However, now the contact area is not compact but instead ring-shaped. The simplest example of such a problem is the contact between a flat, hollow cylindrical punch and the half-space. Even for this simplest of examples, there exists only an extremely complicated solution. Nonetheless, for this class of problems there exists a range of analytical approaches which will be documented in this chapter. These approaches are for the frictionless normal contact with and without adhesion and the non-slipping, purely torsional contact.

10.1 Frictionless Normal Contact without Adhesion

Due to its complexity, the Boussinesq problem of ring-shaped contact areas, i.e., the frictionless normal contact without adhesion between a rigid indenter and an elastic half-space with the effective elasticity modulus E^*, has rarely been considered in literature. Of most practical importance is the case of indenters in the form of hollow cylinders. Some concave rotationally symmetric indenter profiles have been studied as well. The problem here lies in the fact that, for a small normal load and the corresponding ring-shaped contact area, the inner contact radius is unknown and must be determined—as is generally the case for contact problems—as part of the solution. Barber (1974) observed that the current contact area A_c must be the one which maximized the normal force F_N. From the resulting condition

$$\left.\frac{\partial F_N}{\partial A}\right|_{A=A_c} = 0 \tag{10.1}$$

one can determine the contact area if the relationship $F_N(A)$ is known. Barber (1983b) also examined the boundary value problem of a flat-ended cylindrical punch and a central circular recess. Finally, Argatov and Nazarov (1996, 1999) and Argatov et al. (2016) performed a study of toroidal indenters.

V.L. Popov, M. Heß, E. Willert, *Handbook of Contact Mechanics*,
https://doi.org/10.1007/978-3-662-58709-6_10

Support structures are frequently constructed as hollow cylinders to save weight and material. The interior of the hollow cylinder can also be filled with a very soft matrix—similar to bones. The corresponding normal contact problem is considered in Sect. 10.1.1. Some tools feature conical (see Sect. 10.1.2) or parabolic (see Sect. 10.1.3) concave heads, e.g., for stamping purposes. The circular, central recess at the tip of a cylinder (see Sect. 10.1.4) is a classic engineering solution to ensure form-fit connections. The tori examined in Sects. 10.1.5 and 10.1.6 also see wide-spread use. As an example, direct current transformers are increasingly constructed in a toroidal shape instead of the classic E-I design.

10.1.1 The Hollow Flat Cylindrical Punch

The simplest problem considered in this chapter is the normal contact of a flat, hollow cylinder with an elastic half-space. The use of the word "simple" is meant in a relative sense, since even this problem proves to be extremely complex. However, there are a number of solutions to the problem. A schematic diagram of the problem is displayed in Fig. 10.1. Let the cylinder have the outer radius a and the inner radius b and be pressed by the normal force F_N into the half-space to the depth d.

Shibuya et al. (1974) performed a series expansion of the stresses in the contact area $b \leq r \leq a$ proceeding from the singularities at $r = b$ and $r = a$, thereby reducing the problem to an infinite system of coupled linear equations. The coefficients of this system of equations are integrals of a product of four Bessel functions, which does not make the solution particularly easy. Nonetheless, the system can of course be solved numerically and the authors provide a great number of graphical representations of the obtained numerical solutions for the stresses and displacements.

Gladwell and Gupta (1979) made use of an especially elegant superposition of appropriate, known potentials to find an approximate analytical solution of the problem. The potentials result from the solution of the Dirichlet–Neumann problem

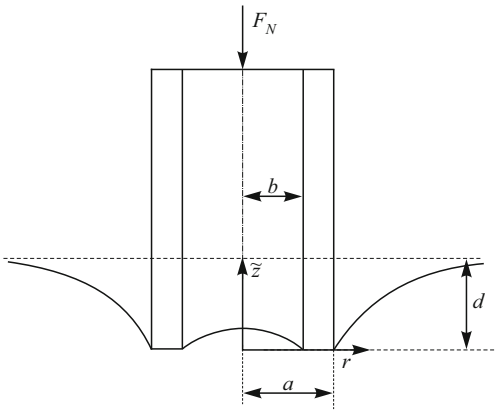

Fig. 10.1 Normal contact of a hollow flat cylinder with an elastic half-space

within and outside the circles $r = b$ and $r = a$. For the relationship between F_N and d they obtain the expression:

$$F_N = 2E^* da\gamma, \tag{10.2}$$

with

$$\gamma = 1 - \frac{4}{3\pi^2}\left(\frac{b}{a}\right)^3 - \frac{1}{8}\left(\frac{b}{a}\right)^4 + O\left[\left(\frac{b}{a}\right)^5\right]. \tag{10.3}$$

The approximation coincides with the ratio of the radii of the exact solution, except for a fourth-order term which is erroneous. The authors also applied their method to the normal contact of a concave paraboloid (see Sect. 10.1.3) and to the Reissner–Sagoci problem for the hollow cylinder (see Sect. 10.3.1).

Using the superposition of harmonic potentials, Gubenko and Mossakovskii (1960) and Collins (1962, 1963) managed to reduce the problem to a Fredholm integral equation, which can be solved iteratively. For γ, Collins found the expression:

$$\gamma = 1 - \frac{4}{3\pi^2}\left(\frac{b}{a}\right)^3 - \frac{8}{15\pi^2}\left(\frac{b}{a}\right)^5 - \frac{16}{27\pi^4}\left(\frac{b}{a}\right)^6 + O\left[\left(\frac{b}{a}\right)^7\right]. \tag{10.4}$$

All series terms given are exactly correct.

Borodachev and Borodacheva (1966a) utilized a similar approach as Collins and determined numerical solutions for the indentation depth $d = d(F_N)$ and the stress $\sigma_{zz} = \sigma_{zz}(r, F_N)$ in a series expansion to the ratio b/a. Borodachev (1976) additionally obtained an asymptotic solution for the stresses in the vicinity of the singularities.

The complete exact solution of the problem was finally worked out by Roitman and Shishkanova (1973), albeit in the form of recursive formulas. Through series expansions and coefficient comparisons they obtained the following expression for the stresses in the contact area:

$$\sigma_{zz}(r; d) = -\frac{E^* d}{2a}\sum_{k=0}^{\infty}\sum_{p=0}^{\infty}\left(\frac{b}{a}\right)^p\left[\alpha_{pk}\left(\frac{r}{a}\right)^{2k} + \beta_{pk}\left(\frac{b}{r}\right)^{2k+3}\right], \tag{10.5}$$

with the recursively determined coefficients

$$\alpha_{pk} = \frac{(2k+1)!!}{(2k)!!}\tilde{\alpha}_{pk}, \quad \beta_{pk} = \frac{(2k+1)!!}{(2k)!!}\tilde{\beta}_{pk},$$
$$\tilde{\alpha}_{0k} = \frac{2}{\pi}\frac{1}{2k+1}, \quad \tilde{\beta}_{0k} = \frac{2}{\pi}\frac{1}{2k+1},$$
$$\tilde{\alpha}_{1k} = \tilde{\alpha}_{2k} = \tilde{\beta}_{1k} = 0, \quad \tilde{\beta}_{2k} = \frac{4}{\pi^2}\frac{1}{3(2k+5)},$$

$$\tilde{\alpha}_{pk} = \frac{2}{\pi}\sum_{q=0}^{I\left(\frac{p-3}{2}\right)}\frac{\tilde{\beta}_{p-2q-3,q}}{2k+2q+3}, \tilde{\beta}_{pk} = \frac{2}{\pi}\sum_{q=0}^{I\left(\frac{p}{2}\right)}\frac{\tilde{\alpha}_{p-2q,q}}{2k+2q+3}, p \geq 3. \tag{10.6}$$

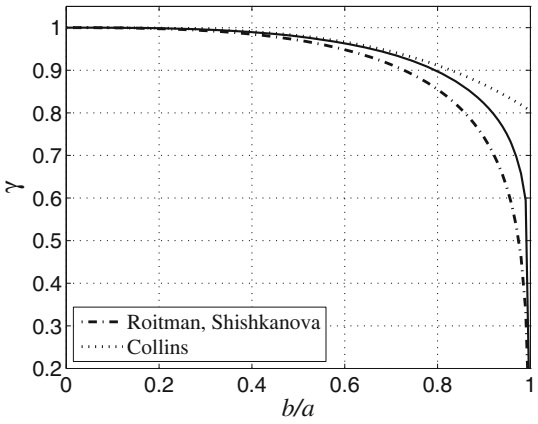

Fig. 10.2 Normalized normal force as a function of the ratio of the radii for a normal contact with a hollow cylindrical punch, according to (10.4) and (10.9). The solid line represents the approximation (10.10)

Here, $(\cdot)!!$ denotes the double faculty

$$n!! := \begin{cases} 2 \cdot 4 \cdot \ldots \cdot n, & n \text{ even}, \\ 1 \cdot 3 \cdot 5 \cdot \ldots \cdot n, & n \text{ odd} \end{cases} \tag{10.7}$$

and $I(x)$ is the largest integer which x does not exceed. For $b = 0$ it returns the familiar result of the flat cylindrical punch:

$$\sigma_{zz}(r; d; b = 0) = -\frac{E^* d}{2a} \sum_{k=0}^{\infty} \alpha_{0k} \left(\frac{r}{a}\right)^{2k} = -\frac{E^* d}{\pi \sqrt{a^2 - r^2}}. \tag{10.8}$$

As expected, the series in (10.5) converges in the open interval $b < r < a$. Term by term integration gives the following expression for γ:

$$\gamma = \frac{\pi}{2} \sum_{k=0}^{\infty} \sum_{p=0}^{\infty} \left(\frac{b}{a}\right)^p \left[\frac{\alpha_{pk}}{2k+2} \left(1 - \left(\frac{b}{a}\right)^{2k+2}\right) + \frac{\beta_{pk}}{2k+1} \frac{b^2}{a^2} \left(1 - \left(\frac{b}{a}\right)^{2k+1}\right) \right]. \tag{10.9}$$

It should be noted that the result for γ in (2.18) of the publication by Roitman and Shishkanova (1973) is incorrect. Grouping the right-hand side of the (10.9) by terms $(b/a)^n$ returns the series expansion from (10.4).

The solutions for γ and the pressure distribution from the (10.9) and (10.5) are shown in Figs. 10.2 and 10.3. The coefficients in (10.6) were evaluated only to $p, k = 150$, with the curve, then scaled to the value $\gamma(b = 0) = 1$.

A closed-form analytical solution was later published by Antipov (1989), the complexity of which would exceed the scope of this handbook. A very good approximation for $\gamma(\varepsilon)$,

$$\gamma(\varepsilon) \approx (1 - \varepsilon^m)^n, \quad m = 2.915; \; n = 0.147 \tag{10.10}$$

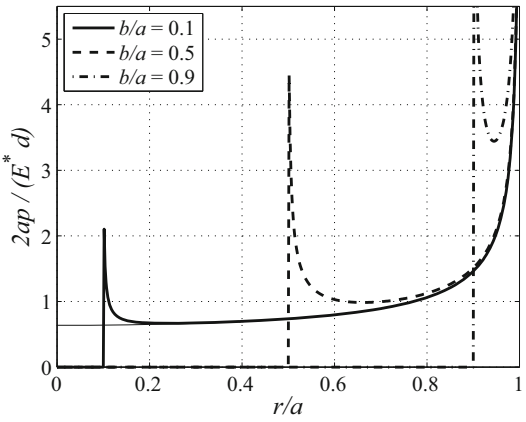

Fig. 10.3 Normalized pressure distribution for a normal contact with a hollow cylindrical punch. The thin solid line represents the solution of the solid cylinder

was given by Willert et al. (2016) on the basis of a very precise boundary element calculation. This is also displayed in Fig. 10.2.

10.1.2 The Concave Cone

The Boussinesq problem of a concave cone was examined by Barber (1976) and Shibuya (1980). A schematic diagram of the problem is shown in Fig. 10.4. Let the base cylinder have the radius a and a concave, conical tip of the depth h. A normal force F_N presses the body into the elastic half-space to the depth d, with the (*a priori* unknown) inner contact radius of b.

Shibuya utilized the same solution approach as in his 1974 publication on the annular punch, i.e., he reduced the problem via a series expansion at the stress singularity at $r = a$ to an infinite system of coupled linear equations and then

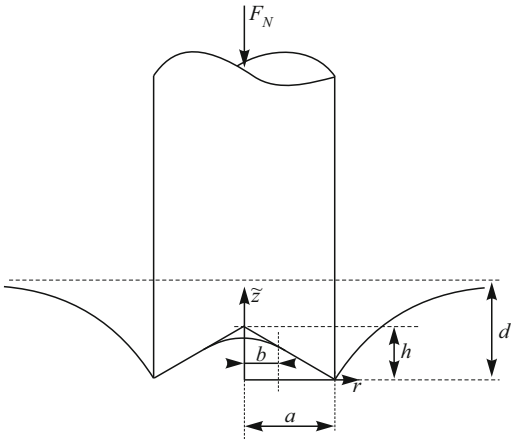

Fig. 10.4 Normal contact of a concave cone with an elastic half-space

solved these numerically. He provided a variety of graphical representations of the numerical solution.

Barber (1976) examined the contact problem in two limiting cases: firstly, for very small values of $\varepsilon = b/a$, and secondly, for the case $\varepsilon \to 1$. For the first approach he used the method by Collins (1963), and for the second approach he used the one by Grinberg and Kuritsyn (1962). For small values of ε, the relationship between F_N, d and ε is given by:

$$F_N(d,\varepsilon) = 2E^* a \left[(d-h)\gamma_1(\varepsilon) + \frac{\pi h}{4}\left(\gamma_2(\varepsilon) - \frac{8\varepsilon^3 \ln \varepsilon}{3\pi^2}\gamma_3(\varepsilon)\right)\right], \tag{10.11}$$

with

$$\begin{aligned}
\gamma_1(\varepsilon) &= 1 - \frac{4\varepsilon^3}{3\pi^2} - \frac{8\varepsilon^5}{15\pi^2} - \frac{16\varepsilon^6}{27\pi^4} - \frac{92\varepsilon^7}{315\pi^2} - \frac{448\varepsilon^8}{675\pi^4} + O(\varepsilon^9),\\
\gamma_2(\varepsilon) &= 1 + \frac{8\varepsilon^3}{9\pi^2} - \frac{52\varepsilon^5}{75\pi^2} - \frac{32\varepsilon^6}{81\pi^4} - \frac{326\varepsilon^7}{735\pi^2} - \frac{496\varepsilon^8}{10125\pi^4} + O(\varepsilon^9),\\
\gamma_3(\varepsilon) &= 1 + \frac{\varepsilon^2}{5} - \frac{4\varepsilon^3}{9\pi^2} + \frac{3\varepsilon^4}{35} - \frac{92\varepsilon^5}{45\pi^2} + O(\varepsilon^6).
\end{aligned} \tag{10.12}$$

The condition stemming from (10.1)

$$\frac{\partial F_N}{\partial \varepsilon} = 0 \tag{10.13}$$

leads to the desired relationship between d and ε,

$$\frac{d}{h} = 1 - \frac{\pi}{4}\frac{\varepsilon^2\gamma_4(\varepsilon) + 2\ln\varepsilon\gamma_5(\varepsilon)}{\gamma_6(\varepsilon)}, \tag{10.14}$$

with

$$\begin{aligned}
\gamma_4(\varepsilon) &= 1 + \frac{16\varepsilon}{81\pi^2} + \frac{5\varepsilon^2}{6} - \frac{14792\varepsilon^3}{10125\pi^2} + O(\varepsilon^4),\\
\gamma_5(\varepsilon) &= 1 + \frac{\varepsilon^2}{3} - \frac{8\varepsilon^3}{9\pi^2} + \frac{\varepsilon^4}{5} - \frac{736\varepsilon^5}{135\pi^2} + O(\varepsilon^6),\\
\gamma_6(\varepsilon) &= 1 + \frac{2\varepsilon^2}{3} + \frac{8\varepsilon^3}{9\pi^2} + \frac{23\varepsilon^4}{45} + \frac{896\varepsilon^5}{675\pi^2} + O(\varepsilon^6).
\end{aligned} \tag{10.15}$$

Figures 10.5 and 10.6 provide a visualization of the shorthand symbols introduced in (10.12) and (10.15).

Greater normal forces cause the radius b to increase and the expression $1-\varepsilon$ to shrink correspondingly. For this case, Barber (1976) gave the following solution for

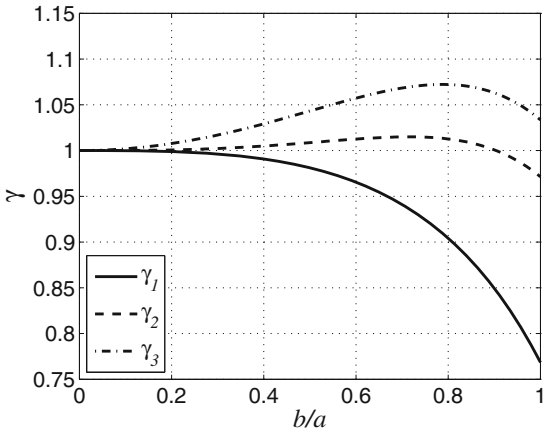

Fig. 10.5 The parameters γ_1 to γ_3 from (10.12) as functions of $\varepsilon = b/a$

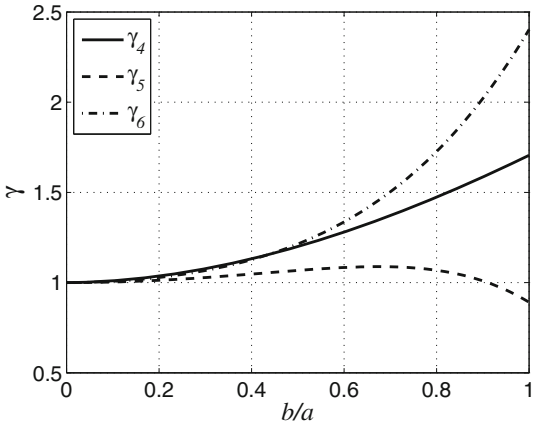

Fig. 10.6 The parameters γ_4 to γ_6 from (10.15) as functions of $\varepsilon = b/a$

the relationship between the global quantities:

$$F_N(d,\delta) = \frac{2\pi^2 E^* a h}{(1+\delta^2)}\left\{\frac{\delta^2}{8} + \left[(1+\delta)\frac{d}{h} - \delta\right]\left[\frac{1}{2L} + \frac{\delta^2}{32}\left(2 - \frac{5}{L} + \frac{4}{L^2}\right)\right]\right\},$$
$$\frac{d}{h} = 1 - \frac{\left[\frac{1}{L} - \frac{3\delta}{2} + \frac{\delta^2}{16}\left(19 - \frac{13}{2L} + \frac{4}{L^2}\right) - \frac{\delta^3}{64}(9 - 6L) + O(\delta^4)\right]}{(1+\delta)\left[\frac{1}{L} - \frac{\delta}{2} + \frac{\delta^2}{16}\left(3 - \frac{13}{2L} + \frac{4}{L^2}\right) - \frac{\delta^3}{64}(3 - 2L) + O(\delta^4)\right]}, \tag{10.16}$$

with the expressions

$$\delta = \frac{1-\varepsilon}{1+\varepsilon},$$
$$L = \ln\frac{16}{\delta}. \tag{10.17}$$

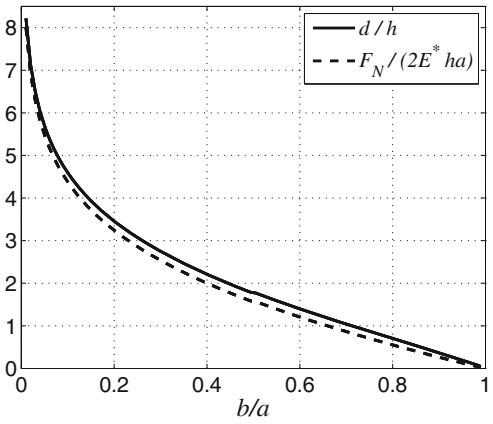

Fig. 10.7 Normalized indentation depth d/h and normal force $F_N/(2E^*ha)$ as functions of $\varepsilon = b/a$ for normal contact with a concave conical indenter

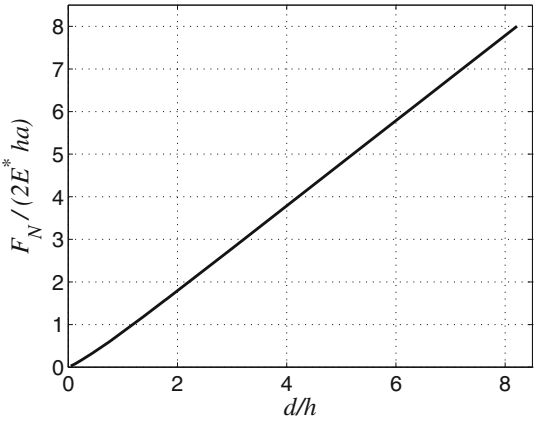

Fig. 10.8 Normalized normal force as a function of the normalized indentation depth for the normal contact with a concave conical indenter

A graphical representation of the relationships between the global contact quantities is given in Figs. 10.7 and 10.8. For $\varepsilon < 0.5$, (10.11) and (10.14) were used; for all others (10.16) was used. They achieve a near perfect match at the transition point $\varepsilon = 0.5$. It can also be seen that, quantitatively, the curves are nearly identical, thus the implicitly given relationship $F_N = F_N(d)$ can be written as:

$$F_N \approx 2E^* da, \tag{10.18}$$

which means that the relationship between the normal force and the indentation depth roughly corresponds to the one of the flat cylindrical punch! The case $b = 0$, i.e., complete contact, is impossible since it would imply an infinitely large normal force.

10.1.3 The Concave Paraboloid

The normal contact with a concave paraboloid was investigated by Barber (1976), Gladwell and Gupta (1979), and Shibuya (1980). Shibuya formulated the problem as a coupled system of infinitely many linear equations and then solved these numerically (see the beginning of the previous section). Gladwell and Gupta utilized an elegant approximation method which relied on a superposition of appropriate potentials (see Sect. 10.1.1). They compared their results to that of Barber's which was the source of the only completely analytical calculations.

A schematic diagram of the contact problem is displayed in Fig. 10.9. Let a flat punch of radius a have a parabolic depression of height h at its tip. Under small loads, the contact area will be ring-shaped with an inner radius b. As already demonstrated in Chap. 2 (see Sect. 2.5.15), fulfilment of the condition

$$d \geq d_c = 3h, \tag{10.19}$$

or alternatively

$$F_N \geq F_c = \frac{16}{3} E^* a h, \tag{10.20}$$

leads to the formation of complete contact ($b = 0$), in which case solution is much simpler. In the following section, we will present the solution of the incomplete contact. Barber (1976) examined, as in the case of the concave conical indenter, the limiting cases $\varepsilon = b/a \to 0$ (using the method of Collins 1963) and $\varepsilon \to 1$ (with the method of Grinberg and Kuritsyn 1962). Small values of ε return the following equations as the solution of the contact problem:

$$\begin{aligned} F_N(d, \varepsilon) &= 2E^* a \left[(d - h)\gamma_1(\varepsilon) + \frac{2h}{3}\gamma_2(\varepsilon) \right], \\ \frac{d}{h} &= 1 + 2\frac{\gamma_3(\varepsilon)}{\gamma_4(\varepsilon)}, \end{aligned} \tag{10.21}$$

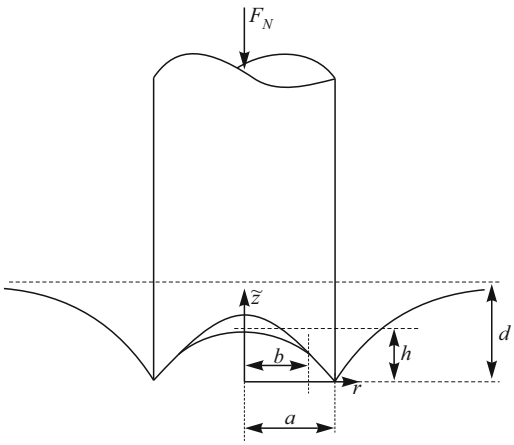

Fig. 10.9 Normal contact of a concave paraboloid with an elastic half-space

with the previously introduced shorthand symbols:

$$\begin{aligned}
\gamma_1(\varepsilon) &= 1 - \frac{4\varepsilon^3}{3\pi^2} - \frac{8\varepsilon^5}{15\pi^2} - \frac{16\varepsilon^6}{27\pi^4} - \frac{92\varepsilon^7}{315\pi^2} - \frac{448\varepsilon^8}{675\pi^4} + O(\varepsilon^9),\\
\gamma_2(\varepsilon) &= 1 + \frac{4\varepsilon^3}{\pi^2} - \frac{8\varepsilon^5}{5\pi^2} - \frac{16\varepsilon^6}{9\pi^4} - \frac{4\varepsilon^7}{5\pi^2} - \frac{32\varepsilon^8}{225\pi^4} + O(\varepsilon^9),\\
\gamma_3(\varepsilon) &= 1 - \frac{2\varepsilon^2}{3} - \frac{8\varepsilon^3}{9\pi^2} - \frac{7\varepsilon^4}{15} - \frac{64\varepsilon^5}{675\pi^2} + O(\varepsilon^6),\\
\gamma_4(\varepsilon) &= 1 + \frac{2\varepsilon^2}{3} + \frac{8\varepsilon^3}{9\pi^2} + \frac{23\varepsilon^4}{45} + \frac{896\varepsilon^5}{675\pi^2} + O(\varepsilon^6)
\end{aligned} \tag{10.22}$$

For values of $\varepsilon \to 1$ we obtain:

$$\begin{aligned}
&F_N(d,\delta) = \\
&\frac{2\pi^2 E^* a h}{(1+\delta^2)}\left\{\frac{\delta^2}{4}\left(1+\frac{1}{L}\right)\right.\\
&\qquad\left.+\left[(1+\delta)^2\left(\frac{d}{h}-1\right)+1\right]\left[\frac{1}{2L}+\frac{\delta^2}{32}\left(2-\frac{5}{L}+\frac{4}{L^2}\right)\right]\right\},\\
&\frac{d}{h} = 1 - \frac{\left[\frac{1}{L}-\frac{5\delta}{2}+\frac{\delta^2}{16}\left(51+\frac{3}{2L}+\frac{4}{L^2}\right)-\frac{\delta^3}{64}(55-10L)+O(\delta^4)\right]}{(1+\delta)^2\left[\frac{1}{L}-\frac{\delta}{2}+\frac{\delta^2}{16}\left(3-\frac{13}{2L}+\frac{4}{L^2}\right)-\frac{\delta^3}{64}(3-2L)+O(\delta^4)\right]},
\end{aligned} \tag{10.23}$$

with the expressions:

$$\begin{aligned}
\delta &= \frac{1-\varepsilon}{1+\varepsilon},\\
L &= \ln\frac{16}{\delta}.
\end{aligned} \tag{10.24}$$

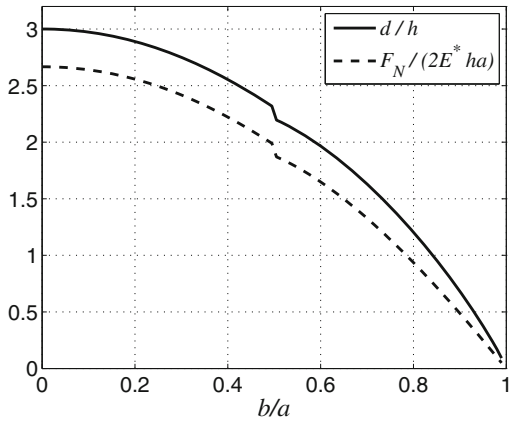

Fig. 10.10 Normalized indentation depth d/h and normalized normal force $F_N/(2E^*ha)$ as functions of $\varepsilon = b/a$ for the normal contact with a concave parabolic indenter. Left-hand side according to (10.21), and right-hand side according to (10.23)

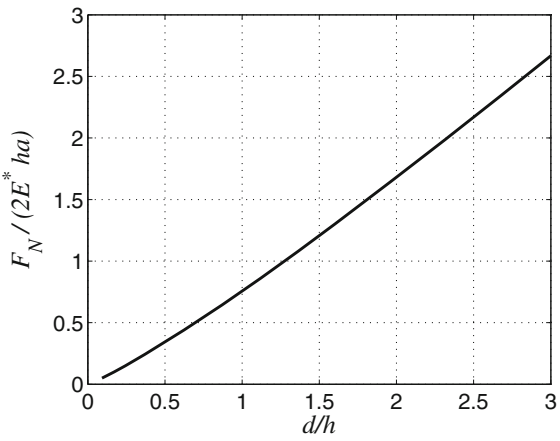

Fig. 10.11 Normalized normal force as a function of the normalized indentation depth for the normal contact of a concave parabolic indenter. Left-hand side according to (10.21), and right-hand side according to (10.23)

Note that (25) of Barber's publication (corresponding to (10.23)) contains a small printing error.

Figures 10.10 and 10.11 offer a visual representation of the relationships between the global contact quantities. For $\varepsilon < 0.5$, (10.21) were used; for all others, (10.23) were used. They achieve quite a good match at the transition point. The limits stated in this section for $b = 0$ are quite clear to see.

10.1.4 The Flat Cylindrical Punch with a Central Circular Recess

To fully understand the line of reasoning present in the literature, and due to the technical importance of this problem, this section is devoted to describing a contact problem that so far has completely evaded an analytical solution. It has even evaded one in the form of integrals, series expansions, or recursions as in the previous sections.

We consider the frictionless normal contact of a flat cylindrical punch of radius a, which features a central circular recess of radius b and depth e. Let the normal force F_N be sufficiently large to form another contact domain in the interior of the recess of radius c (for $c = 0$ it would result in the contact of the annular punch discussed in Sect. 10.1.1). A schematic diagram of the contact problem is given in Fig. 10.12.

This is a four-part boundary value problem, since in the zones $0 \leq r \leq c$ and $b \leq r \leq a$ the displacement are known. In the zones $c < r < b$ and $r > a$ the (vanishing) normal stress are the given values. The problem was considered by Barber (1983b), who reduced it to two coupled Fredholm equations using the method of complex potentials by Green and Collins (see, for example, the preceding publication by Barber 1983a). The equations are then solved numerically. The author provides graphical representations for the normal force and the indentation depth as functions of the contact radius.

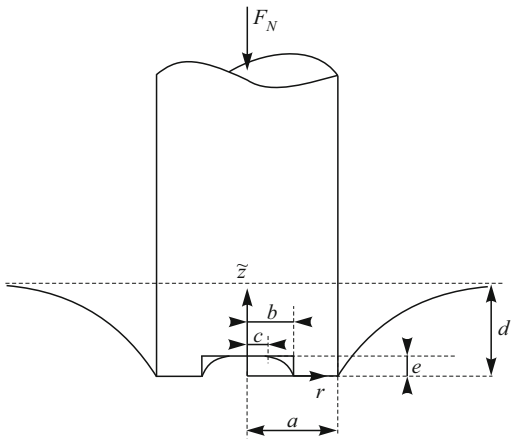

Fig. 10.12 Normal contact of a flat punch with a central recess and an elastic half-space

10.1.5 The Torus

We now consider the frictionless normal contact between a toroidal indenter and an elastic half-space. Let the torus of radii R_1 and R_2 be pressed by a normal force F_N into the elastic half-space to the depth d (see Fig. 10.13).

A ring-shaped contact area of the thickness $2h$ is formed. Argatov and Nazarov (1996, 1999) found the asymptotic solution of this problem for $h \ll R_2$. The relationships between F_N, d, and h are given by:

$$\begin{aligned} F_N &\approx \frac{\pi^2 E^*}{2} \frac{R_2}{R_1} h^2, \\ d &\approx \frac{h^2}{2R_1} \left(\ln \frac{R_2}{h} + 4 \ln 2 + \frac{1}{2} \right). \end{aligned} \tag{10.25}$$

As a first-order approximation, the stress state under the torus (i.e., in the contact area) can be treated as two-dimensional and is given by:

$$\sigma_{zz}(r;h) \approx -\frac{E^* d}{2 \ln(16R_2/h)} \frac{1}{\sqrt{h^2 - (r - R_2)^2}}. \tag{10.26}$$

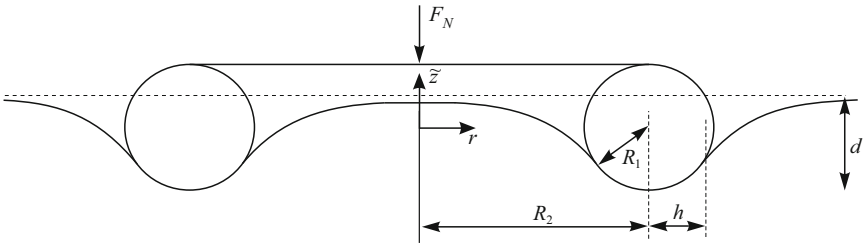

Fig. 10.13 Normal contact (cross-section) between a torus and an elastic half-space

10.1.6 The Toroidal Indenter with a Power-Law Profile

An analogy to the classic torus in the preceding section, the toroidal indenter with an arbitrary profile in the shape of a power-law could also be solved through an asymptotic solution, which was first published by Argatov et al. (2016). A cross-section of the contact problem is given in Fig. 10.14. Let the torus have the radius R and the resulting ring-shaped contact area the width $2h$. The indenter is pressed by a normal force F_N into the half-space to the depth d. The following results are only valid for thin rings; i.e., for $h \ll R$.

Consider an indenter having the rotationally symmetric profile

$$f(r) = c|r - R|^n, \quad n \in \mathbb{R}^+, \tag{10.27}$$

where c is a constant and n a positive real number. The relationship between h and d is given approximately by the expression:

$$d(h) \approx \frac{nch^n}{\kappa(n)} \left(\ln \frac{R}{h} + 4 \ln 2 + \frac{1}{n} \right), \tag{10.28}$$

with the scaling factor from Chap. 2:

$$\kappa(n) := \sqrt{\pi} \frac{\Gamma(n/2 + 1)}{\Gamma\left[(n + 1)/2\right]}. \tag{10.29}$$

Here, $\Gamma(\cdot)$ denotes the Gamma function

$$\Gamma(z) := \int_0^\infty t^{z-1} \exp(-t) \mathrm{d}t. \tag{10.30}$$

The normal force F_N is approximately equal to:

$$F_N(h) \approx \frac{n\pi^2 cRE^*}{\kappa(n)} h^n. \tag{10.31}$$

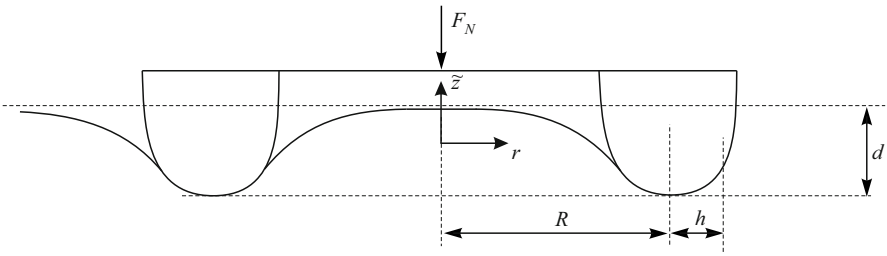

Fig. 10.14 Normal contact (cross-section) between a toroidal body and an elastic half-space

For $n = 2$ and $c = 1/(2R_1)$, we obtain the results of the preceding section. The stress distribution is, in first approximation, two-dimensional and (independent of n) identical to the term in (10.26).

10.1.7 The Indenter Which Generates a Constant Pressure on the Circular Ring

It poses no problem to determine the indenter shape which generates a constant pressure p_0 on the circular ring $b < r < a$. The pressure distribution is a superposition $p(r) = p_1(r) + p_2(r)$ of both distributions

$$\begin{aligned} p_1(r) &= p_0, \quad r < a \\ p_2(r) &= -p_0, \quad r < b. \end{aligned} \tag{10.32}$$

Chap. 2 (Sect. 2.5.6) provides the following displacements of the half-space under the influence of a constant pressure on a circular area of radius a:

$$\begin{aligned} w_1(r; a, p_0) &= \frac{4p_0 a}{\pi E^*} \mathrm{E}\left(\frac{r}{a}\right), \quad r \le a, \\ w_1(r; a, p_0) &= \frac{4p_0 r}{\pi E^*} \left[\mathrm{E}\left(\frac{a}{r}\right) - \left(1 - \frac{a^2}{r^2}\right) \mathrm{K}\left(\frac{a}{r}\right)\right], \quad r > a. \end{aligned} \tag{10.33}$$

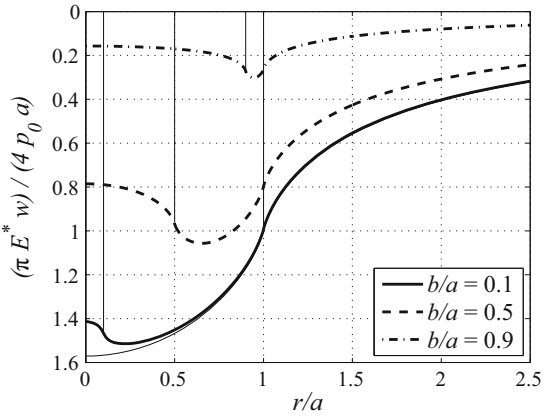

Fig. 10.15 Normalized curve of the half-space displacements under the influence of a constant pressure on a ring-shaped area $b < r < a$ for different ratios of the radii. The thin solid line corresponds to the case $b = 0$

It follows that the displacement under the influence of a constant pressure on a ring-shaped area is:

$$w(r;a,b,p_0) = \frac{4p_0}{\pi E^*}\begin{cases} a\mathrm{E}\left(\frac{r}{a}\right) - b\mathrm{E}\left(\frac{r}{b}\right), & r \le b \\ a\mathrm{E}\left(\frac{r}{a}\right) - r\left[\mathrm{E}\left(\frac{b}{r}\right) - \left(1-\frac{b^2}{r^2}\right)\mathrm{K}\left(\frac{b}{r}\right)\right], & b < r \le a \\ r\left[\mathrm{E}\left(\frac{a}{r}\right) - \left(1-\frac{a^2}{r^2}\right)\mathrm{K}\left(\frac{a}{r}\right) - \mathrm{E}\left(\frac{b}{r}\right)\right. & \\ \quad \left. + \left(1-\frac{b^2}{r^2}\right)\mathrm{K}\left(\frac{b}{r}\right)\right], & r > a. \end{cases} \tag{10.34}$$

These displacements are shown in a normalized representation in Fig. 10.15.

10.2 Frictionless Normal Contact with JKR Adhesion

Ring-shaped contacts also occur in systems which are sufficiently small or soft so that surface forces play a role. One example are hollow ring-shaped positioners in micro-assemblers; such structures are also typical for various biological systems.

As in the compact adhesive contacts, all adhesive models described in Chap. 3 can be applied to ring-shaped contacts, which was the theory of Johnson, Kendall, and Roberts (1971), Maugis (1992), and others. We can also distinguish whether a contact is frictionless or truly *adhesive*, i.e., sticking without tangential slip. We will restrict our consideration to frictionless normal contacts in the JKR approximation. This means that we will assume the range of the adhesive interactions to be small compared to all characteristic lengths of the system. In the JKR approximation, adhesion properties can be completely characterized by the effective surface energy (work of adhesion) per unit area, Δw. The notation Δw used in this chapter differs from the standard notation $\Delta\gamma$ used in all other parts of this book. This is to avoid confusion with the many γ used in the solutions of ring-shaped contacts. Let the half-space have, as always, the effective elasticity modulus E^*.

For contact areas in the form of very thin circular rings, Argatov et al. (2016) presented a very elegant solution for the toroidal indenter in the style of the MDR. It presents the relationships between the global quantities—normal force F_N, indentation depth d, and half of the contact width $h = (a-b)/2$ (with the contact radii b and a)—in the case of the adhesive normal contact. First, the variable

$$\delta = \frac{2h}{a+b} = \frac{a-b}{a+b} \tag{10.35}$$

is introduced, which (in the case of thin circular rings) represents a small parameter. If the adhesion is structured according to the framework of the JKR theory and the relationships of the indentation depth and the normal force of the non-adhesive contact, $d_{\text{n.a.}} = d_{\text{n.a.}}(\delta)$ and $F_{N,\text{n.a.}} = F_{N,\text{n.a.}}(\delta)$, are known, the relationships of the adhesive contact can be obtained through the addition of an appropriate "punch solution".

$$\begin{aligned} d(\delta) &= d_{\text{n.a.}}(\delta) - 2\ln\left(\frac{16}{\delta}\right)\sqrt{\frac{(a+b)\Delta w}{\pi E^*}}\delta, \\ F_N(\delta) &= F_{N,\text{n.a.}}(\delta) - \sqrt{\pi^3(a+b)^3 E^* \Delta w \delta}. \end{aligned} \tag{10.36}$$

The critical state, in which the contact loses its stability and detaches, results from the local maximums of these expressions as functions of δ.

In general though, the solutions are usually only available in the form of asymptotic expansions, which will be presented in the following sections.

10.2.1 The Hollow Flat Cylindrical Punch

Let a hollow flat cylindrical punch with the radii b (inner) and a (outer) be pressed into an elastic half-space. And let adhesion act in the ring-shaped contact area $b \leq r \leq a$ with the effective surface energy Δw. As in the previous sections, we introduce the ratio $\varepsilon = b/a$. The following solution was first presented by Willert et al. (2016).

In Sect. 10.1.1 the following relationship between the normal force $F_{N,\text{n.a.}}$ and the indentation depth d for the non-adhesive contact was derived:

$$F_{N,\text{n.a.}} = 2E^* d a \gamma(\varepsilon). \tag{10.37}$$

Here, the index "n.a." indicates the non-adhesive quantity. The complete expression of the function $\gamma_1(\varepsilon)$ can be referenced in (10.4), (10.9), and (10.10). It should be noted that the two analytical approximations result from series expansions at $\varepsilon = 0$, thus they are only accurate for small values of ε. In Fig. 10.2 a graphical representation of both approximations of the function is given. The elastic energy is then given by:

$$U_{\text{el}} = \int_0^d F_{N,\text{n.a.}}(\delta)\mathrm{d}\delta = E^* d^2 a \gamma(\varepsilon). \tag{10.38}$$

The surface energy, according to the JKR theory, is given by the expression:

$$U_{\text{adh}} = -\Delta w A_c = -\pi \Delta w a^2 \left(1 - \frac{b^2}{a^2}\right) = -\pi \Delta w a^2 \gamma_2(\varepsilon), \tag{10.39}$$

with the contact area A_c. The total potential energy is then:

$$U_{\text{tot}} = E^* d^2 a \gamma(\varepsilon) - \pi \Delta w a^2 \gamma_2(\varepsilon). \tag{10.40}$$

The relation between the normal force and the indentation depth in the adhesive case is then given by:

$$F_N = \frac{\partial U_{\text{tot}}}{\partial d} = 2E^* d a \gamma(\varepsilon) = F_{N,\text{n.a.}}. \tag{10.41}$$

The contact experiences a loss of its stability at:

$$d_c = -\frac{d_0}{\sqrt{\gamma(\varepsilon) - \varepsilon\gamma'(\varepsilon)}}, \tag{10.42}$$

(the prime denotes the derivative with respect to the argument). The corresponding critical normal force, which is also called the adhesive force, is given by:

$$F_c = -\frac{F_0\gamma(\varepsilon)}{\sqrt{\gamma(\varepsilon) - \varepsilon\gamma'(\varepsilon)}}. \tag{10.43}$$

Here the values of the full cylinder, according to Kendall (1971), were used:

$$d_0 := \sqrt{\frac{2\pi a \Delta w}{E^*}}, F_0 := \sqrt{8\pi a^3 E^* \Delta w}. \tag{10.44}$$

Using the results of Collins for $\gamma(\varepsilon)$ (see (10.4)) yields the expression in the denominator:

$$\frac{\varepsilon}{\gamma(\varepsilon)}\frac{\mathrm{d}\gamma}{\mathrm{d}\varepsilon} = -\frac{\frac{4}{\pi^2}\varepsilon^3 + \frac{8}{3\pi^2}\varepsilon^5 + \frac{32}{9\pi^4}\varepsilon^6 + O(\varepsilon^7)}{1 - \frac{4}{3\pi^2}\varepsilon^3 - \frac{8}{15\pi^2}\varepsilon^5 - \frac{16}{27\pi^4}\varepsilon^6 + O(\varepsilon^7)}. \tag{10.45}$$

The Case $\varepsilon \to 1$

As noted in this section, Collins' solution is only usable for small values of ε. For the other limiting case $\varepsilon \to 1$, i.e., with $\delta \to 0$ (δ from (10.35)), the solution by Argatov et al. (2016) can be used.

The relation $F_N = F_{N,\text{n.a.}}$ remains valid of course. Independent of whether a force-controlled or displacement-controlled trial is being conducted, the contact loses its stability at:

$$\begin{aligned} d = d_c &= -2\ln\left(\frac{16}{\delta}\right)\sqrt{\frac{(a+b)\Delta w}{\pi E^*}}\delta, \\ F_N = F_c &= -\sqrt{\pi^3(a+b)^3 E^* \Delta w}\delta. \end{aligned} \tag{10.46}$$

The curves of the critical indentation depth and the adhesive force, both normalized to the values of the solid cylinder, are depicted in Fig. 10.16. For $\varepsilon > 0.85$, the results of (10.46) were used; for all others, (10.42) to (10.45) was used. The values at the transition point are clearly in good agreement. Additionally, the approximate solutions are displayed for which the numerical expression (10.10) was inserted into (10.42) and (10.43).

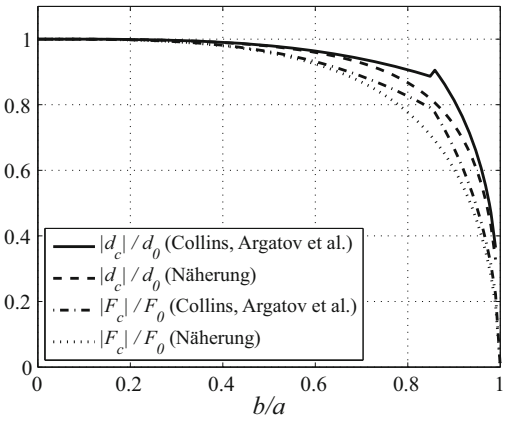

Fig. 10.16 Dependency of the critical indentation depth and adhesive force for the adhesive normal contact with a flat annular punch on $\varepsilon = b/a$. The curves are normalized to the values of the full cylinder ($b = 0$). For $\varepsilon < 0.85$, (10.42), (10.43), and (10.45) were used, and for $\varepsilon > 0.85$, the expressions from (10.46) were used. The smooth transition is clearly visible. The approximate solutions refer to (10.42) and (10.43) with the approximation (10.10)

10.2.2 The Toroidal Indenter with a Power-Law Profile

We consider the adhesive normal contact between a toroidal indenter and an elastic half-space. The indenter has the profile:

$$f(r) = c|r - R|^n, \quad n \in \mathbb{R}^+, \tag{10.47}$$

with a constant c, the radius of the torus R, and a positive real number n. Let the annular contact have the width $2h$ and let the value

$$\delta = \frac{h}{R} \tag{10.48}$$

be small. In this case we can use (10.36). Section 10.1.6 documents the derivation of the following equation for the non-adhesive relationships between the normal force F_N, indentation depth d, and the normalized contact width δ:

$$\begin{aligned} d_{\text{n.a.}}(\delta) &\approx \frac{n c \delta^n R^n}{\kappa(n)} \left[\ln\left(\frac{16}{\delta}\right) + \frac{1}{n} \right], \\ F_{N,\text{n.a.}}(\delta) &\approx \frac{n\pi^2 c E^*}{\kappa(n)} R^{1+n} \delta^n. \end{aligned} \tag{10.49}$$

Here, the index "n.a." indicates the non-adhesive quantities. The function $\kappa(n)$ can be gathered from (10.29). Using (10.36), the adhesive relationships are then given by:

$$\begin{aligned} d(\delta) &\approx \frac{nc\delta^n R^n}{\kappa(n)}\left[\ln\left(\frac{16}{\delta}\right)+\frac{1}{n}\right]-2\ln\left(\frac{16}{\delta}\right)\sqrt{\frac{2R\Delta w}{\pi E^*}}\delta, \\ F_N(\delta) &\approx \frac{n\pi^2 cE^*}{\kappa(n)}R^{1+n}\delta^n-\sqrt{8\pi^3R^3E^*\Delta w\delta}. \end{aligned} \tag{10.50}$$

In a force-controlled trial, the contact experiences a loss of stability at

$$\delta_c{}^{2n-1}=\frac{2}{\pi}\left(\frac{\kappa(n)}{cn^2}\right)^2 R^{1-2n}\frac{\Delta w}{E^*}. \tag{10.51}$$

The corresponding adhesive force has the value

$$F_c=-R\left[\frac{(E^*)^{n-1}(\Delta w)^n\kappa(n)\pi^{3n-2}2^n}{n^{2n+1}c}\right]^{\frac{1}{2n-1}}(2n-1). \tag{10.52}$$

It is obvious that these expressions can be valid only for $n>0,5$. For $n\to\infty$ we obtain the results of the hollow flat cylindrical punch from (10.46). Other special cases which we will briefly examine are:

The V-Shaped Toroidal Indenter with $n=1$
In case of a V-shaped toriidal indenter it is $c=\tan\theta$, with the slope angle θ of the V-profile, $n=1$ and $\kappa(n=1)=\pi/2$. This yields:

$$\begin{aligned} \delta_c &= \frac{\pi}{2\tan\theta}\frac{\Delta w}{RE^*}, \\ F_c &= -R\frac{\Delta w\pi^2}{\tan\theta}. \end{aligned} \tag{10.53}$$

Thus the adhesive force is independent of the elasticity properties of the half-space.

The Classic Torus $n=2$
With $c=1/(2R_1)$, the radius of the torus R_1, $n=2$ and $\kappa(n=2)=2$, we obtain:

$$\begin{aligned} \delta_c &= \sqrt[3]{\frac{1}{\pi R_1}\frac{\Delta w}{R^3E^*}}, \\ F_c &= -3R\sqrt[3]{\left(\frac{R_1E^*(\Delta w)^2\pi^4}{2}\right)}. \end{aligned} \tag{10.54}$$

10.3 Torsional Contact

The purely torsional contact problem between a rigid indenter and an elastic half-space is also referred to as the Reissner–Sagoci problem. The boundary conditions at the surface of the half-space at $z = 0$, in the axisymmetric case for a ring-shaped contact area with the radii b and $a > b$, are as follows:

$$\begin{aligned} u_\varphi(r, z = 0) &= f(r), \quad b \le r \le a, \\ \sigma_{\varphi z}(r, z = 0) &= 0, \quad r < b, r > a, \end{aligned} \tag{10.55}$$

with the rotational displacement and the tangential stresses. This consideration only deals with the pure torsion problem without slip, which means that all other stresses and displacements vanish.

10.3.1 The Hollow Flat Cylindrical Punch

In drilling applications, sometimes hollow or concave drill bits are used. This approximately corresponds to the contact problem described in this section. For the contact of a hollow flat cylindrical punch, the function $f(r)$ of the torsional displacement is given by:

$$f(r) = \varphi r, \tag{10.56}$$

with the twisting angle φ of the punch around its axis of symmetry. The contact problem was studied by Borodachev and Borodacheva (1966b), Shibuya (1976), and Gladwell and Gupta (1979).

Borodachev and Borodacheva (1966b) applied the same method which Collins (1962, 1963) utilized for the solution of the normal contact problem of a flat annular punch. They numerically solved the Fredholm equation that arose over the course of the solution process and obtained the following relationship between the torsional moment M_z and the torsion angle φ:

$$M_z = \frac{16}{3} G a^3 \varphi \gamma(\varepsilon), \tag{10.57}$$

once again introducing the shorthand notation $\varepsilon = b/a$. G is the shear modulus of the elastic half-space. A series expansion of the function $\gamma(\varepsilon)$ is only possible for small values of ε. The authors presented the approximate solution:

$$\gamma = 1 + 0.0094\varepsilon^4 - 0.1189\varepsilon^5 - 0.0792\varepsilon^7 - 0.0094\varepsilon^8 - 0.0645\varepsilon^9 + O(\varepsilon^{10}). \tag{10.58}$$

For the stresses in the contact area they provided the expression:

$$\begin{aligned} \sigma_{\varphi z}(r) \approx -\frac{4G\theta}{\pi} \Bigg\{ & \frac{r}{\sqrt{a^2 - r^2}} \left[1 + \frac{\varepsilon^5}{\pi^2} \left(\alpha_0 + \alpha_2 \frac{r^2}{a^2} + \alpha_4 \frac{r^4}{a^4} + \alpha_6 \frac{r^6}{a^6} \right) \right] \\ & + \frac{\varepsilon b^4}{\pi r^3 \sqrt{r^2 - b^2}} \left(\beta_0 + \beta_2 \frac{b^2}{r^2} + \beta_4 \frac{b^4}{r^4} + \beta_6 \frac{b^6}{r^6} \right) \Bigg\}, \end{aligned} \tag{10.59}$$

with the shorthand notation:

$$\begin{aligned}
\alpha_0 &= 0.0839 + 0.0913\varepsilon^2 + 0.0929\varepsilon^4 + 0.0007\varepsilon^5 + 0.1469\varepsilon^6,\\
\alpha_2 &= 0.0531 + 0.0698\varepsilon^2 + 0.101\varepsilon^4,\\
\alpha_4 &= 0.0434 + 0.0844\varepsilon^2, \quad \alpha_6 = 0.0579,\\
\beta_0 &= 0.2896 + 0.0917\varepsilon^2 + 0.0562\varepsilon^4 + 0.0025\varepsilon^5 + 0.0625\varepsilon^6,\\
\beta_2 &= 0.2083 + 0.075\varepsilon^2 + 0.05\varepsilon^4,\\
\beta_4 &= 0.15 + 0.1\varepsilon^2, \quad \beta_6 = 0.2.
\end{aligned} \tag{10.60}$$

Gladwell and Gupta (1979) solved the contact problem in a very elegant manner through a combination of appropriate potentials. They gave the sought stresses and displacements inside and outside the contact area as:

$$\begin{aligned}
u_\varphi(r) &= \varphi a \begin{cases}
\dfrac{r}{a} - 2b_1 \dfrac{r}{b}\sqrt{1-\dfrac{r^2}{b^2}}, & 0 < r < b\\
\dfrac{r}{a}, & b \le r \le a\\
\dfrac{2r}{\pi a}\left[\arcsin\left(\dfrac{a}{r}\right) - \dfrac{a}{r}\sqrt{1-\dfrac{a^2}{r^2}}\right] & \\
\quad - 6a_1\dfrac{a^2}{r}\sqrt{1-\dfrac{a^2}{r^2}}, & r > a,
\end{cases}\\
\sigma_{\varphi z}(r) &= G\varphi\left[\frac{4r}{\pi a}R\left(\frac{r}{a}\right) - \frac{9b_1 r}{\varepsilon b}U\left(\frac{b}{r}\right) - 9a_1\frac{a^4}{r^4}U\left(\frac{r}{a}\right)\right],\\
&\qquad b \le r \le a,
\end{aligned} \tag{10.61}$$

with the functions U and R and the shorthand notations defined as follows:

$$\begin{aligned}
U(x) &= \begin{cases}
\arcsin x - \dfrac{x}{\sqrt{1-x^2}}\left(1-\dfrac{x^2}{3}\right), & x < 1\\
\dfrac{\pi}{2}, & x \ge 1,
\end{cases}\\
R(x) &= \begin{cases}
\dfrac{1}{\sqrt{1-x^2}}, & x < 1\\
0, & x \ge 1,
\end{cases}\\
b_1 &= \frac{600\varepsilon^2}{675\pi^2 - 48\varepsilon^5}, \quad a_1 = \frac{4\varepsilon^3 b_1}{15\pi} = \frac{160\varepsilon^5}{675\pi^3 - 48\pi\varepsilon^5},
\end{aligned} \tag{10.62}$$

which is in very good agreement with the results of Shibuya (1976), who converted this problem into a coupled system of infinitely many linear equations and solved these numerically.

If we then determine the torsional moment via integration of the stress distribution (this step was not performed in the publication by Gladwell and Gupta) and

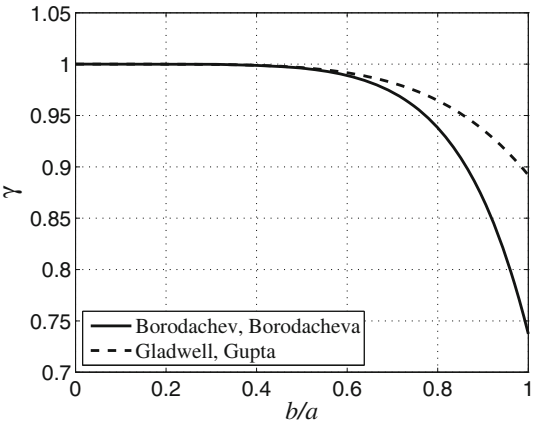

Fig. 10.17 Normalized torsional moment $\gamma = 3M_z/16G\varphi a^3$ as a function of the ratio of radii $\varepsilon = b/a$ according to (10.58) (Borodachev and Borodachev 1966b) and (10.63) (Gladwell and Gupta 1979)

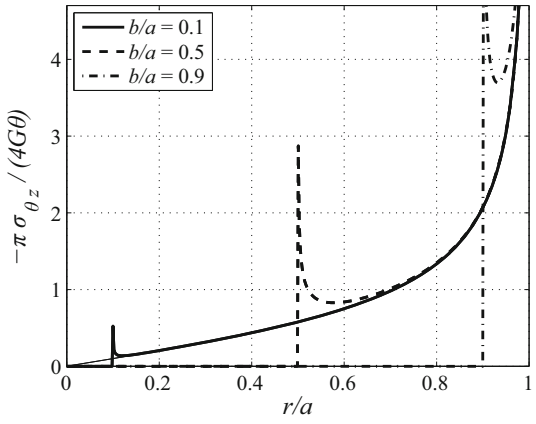

Fig. 10.18 Normalized torsional stresses according to Borodachev and Borodachev (1966b) as a function of the radial coordinate for different values of b/a. The thin solid line represents the solution of the full cylinder

expand the expression for γ in Taylor series to powers of ε we obtain:

$$\gamma = 1 - \frac{16}{15\pi^2}\varepsilon^5 + O(\varepsilon^6). \tag{10.63}$$

Figure 10.17 shows the solutions for γ, according to Borodachev and Borodacheva (1966b) and Gladwell and Gupta (1979). For values of $\varepsilon < 0.6$ they are in very good agreement. We must keep in mind that both solutions are intended only for small values of ε. Figures 10.18 and 10.19 display the solution for the tangential stress distribution on the basis of (10.59) and (10.61). The stress singularities at the sharp edges of the indenter and the convergence with the solution for the flat cylindrical punch from Chap. 5 (see Sect. 5.1.1) are easily recognized.

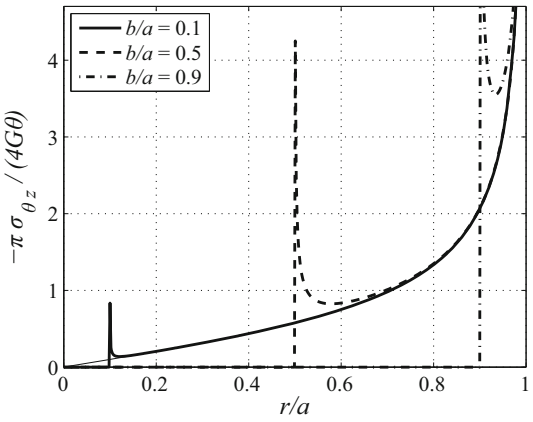

Fig. 10.19 Normalized torsional stresses according to Gladwell and Gupta (1979) as a function of the radial coordinate for different values of b/a. The thin solid line represents the solution of the full cylinder

References

Antipov, Y.A.: Analytic solution of mixed problems of mathematical physics with a change of boundary conditions over a ring. Mech. Solids **24**(3), 49–56 (1989)

Argatov, I.I., Nazarov, S.A.: The pressure of a narrow ring-shaped punch on an elastic half-space. J. Appl. Math. Mech. **60**(5), 799–812 (1996)

Argatov, I.I., Nazarov, S.A.: The contact problem for a narrow annular punch. Increasing contact zone. In: Studies in elasticity and plasticity, pp. 15–26. University Press, St. Petersburg (1999)

Argatov, I.I., Li, Q., Pohrt, R., Popov, V.L.: Johnson–Kendall–Roberts adhesive contact for a toroidal indenter. Proc. R. Soc. London Ser. A **472**, 20160218 (2016). https://doi.org/10.1098/rspa.20160218

Barber, J.R.: Determining the contact area in elastic indentation problems. J. Strain Anal. **9**(4), 230–232 (1974)

Barber, J.R.: Indentation of the semi-infinite elastic solid by a concave rigid punch. J. Elast. **6**(2), 149–159 (1976)

Barber, J.R.: The solution of elasticity problems for the half-space by the method of Green and Collins. Appl. Sci. Res. **40**(2), 135–157 (1983a)

Barber, J.R.: A four-part boundary value problem in elasticity: indentation by a discontinuously concave punch. Appl. Sci. Res. **40**(2), 159–167 (1983b)

Borodachev, N.M.: On the nature of the contact stress singularities under an annular Stamp. J. Appl. Math. Mech **40**(2), 347–352 (1976)

Borodachev, N.M., Borodacheva, F.N.: Penetration of an annular stamp into an elastic half-space. Mech. Solids **1**(4), 101–103 (1966a)

Borodachev, N.M., Borodacheva, F.N.: Twisting of an elastic half-space by the rotation of a ring-shaped punch. Mech. Solids **1**(1), 63–66 (1966b)

Collins, W.D.: On some triple series equations and their applications. Arch. Ration. Mech. Anal. **11**(1), 122–137 (1962)

Collins, W.D.: On the solution of some Axi-symmetric boundary value problems by means of integral equations. VIII. Potential problems for a circular annulus. Proc. Edinb. Math. Soc. Ser. 2 **13**(3), 235–246 (1963)

Gladwell, G.M.L., Gupta, O.P.: On the approximate solution of elastic contact problems for a circular annulus. J. Elast. **9**(4), 335–348 (1979)

Grinberg, G.A., Kuritsyn, V.N.: Diffraction of a plane electromagnetic wave by an ideally conducting plane ring and the electrostatic problem for such a ring. Soviet Phys. Tech. Phys. **6**, 743–749 (1962)

Gubenko, V.S., Mossakovskii, V.I.: Pressure of an axially-symmetric circular die on an elastic half-space. J. Appl. Math. Mech **24**(2), 477–486 (1960)

Johnson, K.L., Kendall, K., Roberts, A.D.: Surface Energy and the Contact of Elastic Solids. Proc. Royal Soc. Lond. Ser. A **324**, 301–313 (1971)

Kendall, K.: The adhesion and surface energy of elastic solids. J. Phys. D Appl. Phys. **4**(8), 1186–1195 (1971)

Maugis, D.: Adhesion of spheres: The JKR-DMT-transition using a Dugdale model. J. Colloid Interface Sci. **150**(1), 243–269 (1992)

Roitman, A.B., Shishkanova, S.F.: The solution of the annular punch problem with the aid of Recursion relations. Soviet Appl. Mech. **9**(7), 725–729 (1973)

Shibuya, T.: A mixed boundary value problem of an elastic half-space under torsion by a flat annular rigid stamp. Bull. JSME **19**(129), 233–238 (1976)

Shibuya, T.: Indentation of an elastic half-space by a concave rigid punch. Z. Angew. Math. Mech. **60**(9), 421–427 (1980)

Shibuya, T., Koizumi, T., Nakahara, I.: An elastic contact problem for a half-space indented by a flat annular rigid stamp. Int. J. Eng. Sci. **12**(9), 759–771 (1974)

Willert, E., Li, Q., Popov, V.L.: The JKR-adhesive normal contact problem of Axi-symmetric rigid punches with a flat annular shape or concave profiles. Facta Univ. Seri. Mech. Eng. **14**(3), 281–292 (2016)